MODELLING AND DIMENSIONING A HOT WATER FLOOR HEATING SYSTEM

D. CACCAVELLI(*) ; B. BEDOUANI(*) & J. BAUDE(**)

(*) Centre Scientifique et Technique du Bâtiment
Service Génie Energétique et Climatique
84 avenue Jean Jaurès - BP 02
77421 MARNE-la-VALLEE, France

(**) Gaz-de-France
Centre d'Essais et de Recherches
sur les Utilisations du Gaz
361 avenue du Président Wilson, BP 33
93210 LA PLAINE-SAINT-DENIS, France

ABSTRACT

The Centre Scientifique, et Technique du Bâtiment and Gaz-de-France carried out a comprehensive study for providing professionals with dimensioning rules for hot water floor heating systems.

In the first phase we used a general purpose finite element analysis program called MARC and developed a three-dimensional mesh integrating the different floor heating components.

In a second phase, simulation results were compared to an experimental result data set created for this study from a test cell specially dedicated to heating floor assessment.

Finally, the numerical model was compared and validated against experimental results in both steadystate and dynamic regime.

INTRODUCTION

The constant decrease in heating loads induced by the improvement of building thermal performances, the application of new standards such as acoustic (which made necessary the use of floating concrete slab in multi-storey buildings), have boosted the hot water floor heating market.

In order to avoid repeating the errors which at the end of the sixties nearly discredited this heating technique, the Centre Scientifique et Technique du Bâtiment (Scientific and Technical Building Centre) and Gaz-de-France (French gas supply company) carried out a comprehensive study for providing professionals with dimensioning rules for hot water floor heating systems. These rules are based on the strict compliance with thermal comfort conditions (French regulations limit the maximum floor surface temperature to 28°C for a standard indoor room temperature of 19°C).

NUMERICAL APPROACH

We used a general purpose finite element analysis program called MARC [1] to model the coupled problem of heat conduction in solid type structure (heating floor) and convective heat transfer in the fluid channel (heating pipe).

The numerical technique used in MARC is based on a finite element approximation scheme derived from the Galerkin version of the method of weighted residuals which was applied by ZIENKIEWICZ and PAREKH [2].

MATHEMATICAL FORMULATION OF HEAT CONDUCTION PROBLEM IN SOLID

Consider a structure of volume V and surface Γ which is subjected to a heat flow varying in time. From the conservation of energy principle, a parabolic differential equation can be derived expressing the balance of heat within volume V for all times:

$$(1)\ \iiint_V \left[\frac{\partial}{\partial x_i}\left(\lambda_{ij} \frac{\partial T}{\partial x_j} \right) + Q_{int} - \rho \cdot c \cdot \frac{\partial T}{\partial t} \right] d = 0$$

Where:

- T = Temperature; K
- Q_{int} = Rate of heat production per unit volume; W/m^3
- ρ = Mass density per unit volume; kg/m^3
- c = Specific heat; J/kg.K
- $\lambda_{i,j}$ = Thermal conductivity in the distinct spatial directions; W/m.K

Using the finite element approximation scheme, the overall temperature distribution is approximated by a finite number of simple shaped temperature distributions within the elements, as follows:

$$(2) \qquad \tilde{T}(x_i,t) = \sum_{i=1}^{n} N_i(x_i).T_i(t) = N^T.T$$

Where:

N = Vector of shape functions.
T = Vector of time-dependent nodal point temperatures.
n = Number of nodes of element.

When the weighted residual-Galerkin concept is applied, the following system of finite element equations is obtained:

$$(3) \qquad C.T + (K+F).T = Q$$

The matrix C is the so-called heat capacity matrix. It is related to the storage of heat in each element during a transient heat transfer process:

$$(4) \qquad C = \sum_{\text{éléments}} \iiint_{V^e} \rho.c.N^T.N\,dv$$

The matrix K is the so-called conductivity matrix. It is related to the heat conduction effects in each element.

(5)

$$K = \sum_{\text{éléments}} \iiint_{V^e} \left[\lambda_x \frac{\partial N}{\partial x}\frac{\partial N^T}{\partial x} + \lambda_y \frac{\partial N}{\partial y}\frac{\partial N^T}{\partial y} + \lambda_z \frac{\partial N}{\partial z}\frac{\partial N^T}{\partial z} \right] dv$$

The vector Q is the nodal heat flux vector which consists of the following contributions:

$$(6) \qquad Q = \sum_{\text{éléments}} \left(\iiint_{V^e} N.Q_{int}.dv + \iint_{\Gamma_2^e} N.\varphi ds + \iint_{\Gamma_3^e} h.N.T_\infty ds \right)$$

Where φ denotes a boundary condition of the Neumann type, h is the coefficient of surface heat transfer and T_∞ is the reference temperature of the outer medium.

Finally, the form of matrix F is similar to the heat capacity matrix C:

$$(7) \qquad F = \sum_{\text{éléments}} \iint_{\Gamma_3^e} h.N.N^T ds$$

In steady-state regime, equation (3) is reduced to:

$$(8) \qquad (K+F).T = Q$$

In transient regime, a backward difference method is used and T_n is approximated by:

$$(9) \qquad T_n = \frac{1}{\Delta t}.(T_n - T_{n-1})$$

Where Δt is the time-step.

Replacing equation (9) with equation (3) yields:

$$(10) \qquad \left(C + \Delta t.(K+F)\right).T_n = C.T_{n-1} + \Delta t.Q_n$$

MATHEMATICAL FORMULATION FOR CONVECTIVE HEAT TRANSFER PROBLEMS IN PIPE

Several two-and three-dimensional MARC heat transfer elements are designed for the modelling of convective heat transfer in fluid channel (heating or cooling pipe).

They are based on the following assumptions:

- heat conduction in the flow direction can be neglected compared to heat convection,
- the heat flux associated with transient effects in the fluid can be neglected.

The one-dimensional, steady state, convective heat transfer in the fluid channel can thus be expressed as:

$$(11) \qquad Q_f.Cp_f\frac{\partial T_f}{\partial z} + h_f S.(T_f - T_s) = 0$$

Where:

Q_f = Fluid mass flow rate; kg/s
C_{pf} = Fluid specific heat; J/kg.K
T_f = Fluid temperature; K
h_f = Heat transfer coefficient; $W/m^2.K$
S = Circumference of channel; m
T_s = Channel surface temperature; K

EXPERIMENTAL APPROACH

Test room:

All the tests were carried out in a high-insulated climatic test cell, located at the CSTB in Marne-la-Vallée, where ambient conditions are controled (see figure 1). This experimental set up enables to test under artificial conditions removable full-scale floors.

The heat losses from the cell are simulated by air, injected at slow speed, through a plenum.

The air inflow temperature is controled in such a way that the indoor air temperature of the cell will be permanently from 18°C to 20°C.

The hot water production system was designed in such a way that the supply temperature and the fluid flow would be as stable as possible.

Test bench :

a) Description of the heating floor.

The floor, dimensions 3m x 3m, rests on a wood support, mounted on rollers.

The heating pipes (HDP) are fixed to thermal insulating panels with individual attachment studs and are completely embedded in the reinforced concrete slab (see figure 2).

Attaching systems raise the base of the heating pipes 15 mm above the plane of the insulation.

b) Laying of piping.

The heating pipes are distributed in the test bench in order to constitute seven identical rows, mounted in parallel on the distribution circuits (see figure 3).

An individual balancing system with flow regulating valves located on the distribution circuits, makes it possible to adjust to an identical water flow in each of the rows.

c) Instrumentation.

The central row of the test bench is finely instrumented in three main zones:

two peripheral zones, located on either side of the edges of the heating floor (zones 1 and 3),
one central zone (zone 2).

Each zone receives instrumentation next to the supply and return pipes as well as between the heating pipes (see figure 3).

The heating floor is instrumented on five different The heating floor is instrumented on five different planes:

- floor covering surface,
- concrete surface,
- upper surface of heating pipe,
- lower surface of heating pipe,
- surface of insulation.

To complete this instrumentation, an infrared motion picture camera was used. This camera provides precise mapping of the temperatures at the surface of the floor.

VALIDATION

We compared the numerical results predicted by the MARC program to the experimental results obtained during the various tests.

Conditions :

a) Study field.

The test bench includes a large dimension floor. Given the symetries induced by the laying of piping the problem's study field can be reduced. Because of this, the comparisons concern only the central row.

b) Finite element discretization.

The solid type structure (heating floor) has been discretized using eight-noded, isoparametric, three-dimensional brick elements (see figure 4).

Either the coordinate or temperature approximation $\approx$
T can be expressed in terms of the nodal quantities by the integration functions:

$$(11)\quad \begin{cases} x = \sum_{i=1}^{8} x_i \Phi_i \\ y = \sum_{i=1}^{8} y_i \Phi_i \\ z = \sum_{i=1}^{8} z_i \Phi_i \\ \overset{\approx}{T} = \sum_{i=1}^{8} T_i \Phi_i \end{cases}$$

$$\Phi_1 = \frac{1}{8}(1-\xi)(1-\eta)(1-\zeta) \qquad \Phi_5 = \frac{1}{8}(1-\xi)(1-\eta)(1+\zeta)$$

$$\Phi_2 = \frac{1}{8}(1+\xi)(1-\eta)(1-\zeta) \qquad \Phi_6 = \frac{1}{8}(1+\xi)(1-\eta)(1+\zeta)$$

$$\Phi_3 = \frac{1}{8}(1+\xi)(1+\eta)(1-\zeta) \qquad \Phi_7 = \frac{1}{8}(1+\xi)(1+\eta)(1+\zeta)$$

$$\Phi_4 = \frac{1}{8}(1-\xi)(1+\eta)(1-\zeta) \qquad \Phi_8 = \frac{1}{8}(1-\xi)(1+\eta)(1+\zeta)$$

c) Mesh generation.

A three-dimensional mesh has been generated for the purpose of analysis. The mesh is made up of 2570 eight-noded heat transfer elements (see figure 5).

d) Boundary conditions.

We applied boundary conditions of the Fourier type on horizontal surfaces of the heating floor:

$$\iint_{\Gamma_3} -\lambda_n \frac{\partial T}{\partial n}\, ds = \iint_{\Gamma} h.(T - T_\infty) ds$$

The coefficient of surface heat transfer, h, can be calculated as follows :

(13) $$h = h_r + h_c$$

Where:

h_r = Radiative heat transfer coefficient; $W/m^2.K$

h_c = Convective heat transfer coefficient; $W/m^2.K$

The radiative coefficient is assumed to be constant. It has been evaluated at:

(14) $$h_r = 5.9\ W/m^2.K$$

The following expressions are used to evaluate the heat transfer coefficient for convection:

* horizontal surface facing upward [3]:

(15) $$h_c = 1.50\,|T-T_\infty|^{0.33}\ (W/m^2.K)$$

* horizontal surface facing downward [4]:

(16) $$h_c = 1\ (W/m^2.K)$$

At the interface between the fluid and the heating pipe, the heat flux estimated from convective heat transfer is :

(17) $$\iint_{pipe} -\lambda_n \frac{\partial T}{\partial n} \cdot ds = h_f \cdot \iint_{pipe} (T_s - T_f) \cdot ds$$

The heat transfer coefficient h_f could be calculated using the following empirical law [5] :

(18) $$h_f = 1.75 \cdot \frac{\lambda_f}{\phi_i} \left(\frac{Q_f \cdot Cp_f}{\lambda_f \cdot L} \right)^{0.33}$$

Where L is the length of the pipe from which the assumption of a uniform fluid temperature is correct and λ_f the fluid thermal conductivity.

Results:

a) Steady-state analysis.

The simulations were carried out while setting the values of a certain number of inputs to the model:

- Flow rate of fluid circulating in the central row,
- Flow supply temperature,
- Indoor air temperature of the room,
- Resulting dry bulb temperature under the floor.

These values correspond to the values measured during the various tests.

Figures 6 and 7 display a part of the results of this comparison. The analysis of these results, in steady-state brings out the following tendencies:

The differences observed between the model's predictions and the experiments are small at the surface of the insulation. The maximal difference observed for all the simulations is 0.6°C, which is located within the measurement's uncertainty range.

At the surface of the floor, the differences found are greater. The maximal difference observed is approximately 1°C.

The difference between the temperatures at the surface of the floor, calculated and measured, is particularly large at the level of the first peripheral zone (zone 1) and tends to become smaller for the two following zones (zones 2 and 3).

We have searched for reasons for such behaviour. To do this, we used the results supplied by an infrared motion picture camera which makes it possible to gather more complete information for the temperatures obtained at the surface of the floor.

On figure 8, we plotted the evolution of the temperature range measured at the surface of the floor along the axis of the pipe, next to the return pipe.

The pattern of points obtained demonstrates a strange behaviour which can only be explained by the sagging of the pipe. To support this explanation, we noted on this diagram the exact locations of the attachment studs which raise the pipe at a certain height (15 mm). We found that the surface temperature is maximal at the locations of these studs and that it fluctuates between two consecutive studs. It therefore would seem that, under the weight of the concrete that the pipe did not remain horizontal (assumption adopted during the modelling), but deviated. We also remark that the magnitude of the oscillations decreases as we move further away from the edge of the floor. This is explained by a reduction in the spacing of the attachments (as we come closer to the pipe loop, the number of attachments was increased).

Onto this diagram we have superposed the numerical results predicted by the model. At the attaching points, we see that the differences between the numerical values and the experimental values obtained by infrared camera are very small (a maximum of 0.2°C).

To conclude, wherever we can guarantee a known position of the pipe (this is the case at the attaching points), we observe a good agreement between numerical results and experimental results.

b) Transient analysis.

Two tests were carried out:

- short duration start/stop cycles of the fluid circulating pump (alternating start/stop cycles of 30 min each).

- long duration start/stop cycles of the fluid circulating pump (10 hours off followed by 14 hours on).

Unlike the tests performed in steady-state where a single value is enough to define each of the model's inputs, in transient, the inputs vary with time. These inputs are therefore read in a data file.

Figures 9a and 9b display a part of the results of this comparison. The analysis of these results, in transient brings out the following tendencies:

- The dynamic of the phenomena observed experimentally is accurately reproduced by the numerical model.

- The effects of the deflection of the heating pipes also appear in these simulations whenever the fluid circulating pump is running (and, to a lesser degree, whenever the pump is off).

- Whenever the fluid circulating pump is stopped (off) we observe an increase in the temperature differences, the temperature measured then being (whatever the measurement) always above the corresponding calculated temperature. This is related to the hypotheses decided upon for modelling the fluid flow in the pipe, that is:

  * no transient effects in pipe,

  * no heat conduction in the flow direction.

In any event, the differences observed remain quite acceptable and do not bring the hypotheses fundamentally into question.

CONCLUSION

Unlike a theoretical approach, like the one developed in the sixties in France by CLAIN and CADIERGUES [6], a numerical approach is only meaningful if the predicted results are able to be successfully compared with the experimental results.

For this reason, the model used for this study was subjected to many validation tests both in steady-state and transient modes.

This procedure indicates that:

- the numerical model used is completely suitable for correctly re-expressing the thermal phenomena observed experimentally, both from a qualitative and quantitative point of view, for steady-state and for transient modes,

- the differences observed are due to comparative conditions which differ slightly from the test model (position of the heating pipe).

Finally, we should note that from this study , we have also derived a major experimental knowledge base concerning the thermal behaviour of floors with hot water underfloor heating, a knowledge base which will be able to serve for validating any other model.

REFERENCES

[1] F.J.H. PEETERS and A.W.A. KONTER
"Heat transfer and thermal stress analysis using MARC"
MARC Analysis Research Corporation, March 1991.

[2] O.C. ZIENKIEWICZ and C.J. PAREKH
"Transient field problems : Two-dimensional and three-dimensional analysis by isoparametric finite elements"
Int. J. Num. Meth. Eng., 2, pp 61-71, 1970.

[3] J.F. SACADURA
Initiation aux transferts thermiques.
Paris, Lavoisier, 1982, 446 p.

[4] D. CACCAVELLI and P. RICHARD
"Etude portant sur le dimensionnement d'un plancher chauffant à eau chaude en CIC."
Rapport n°2, CSTB, n° GEC/DST-94.050R, Juillet 1994

[5] W.H. Mac ADAMS
Transmission de la chaleur.
Paris, Dunod, 1950, 537 p.

[6] F. CLAIN and R. CADIERGUES
Nouvelles données sur les panneaux incorporés.
Industries thermiques, Décembre 1962

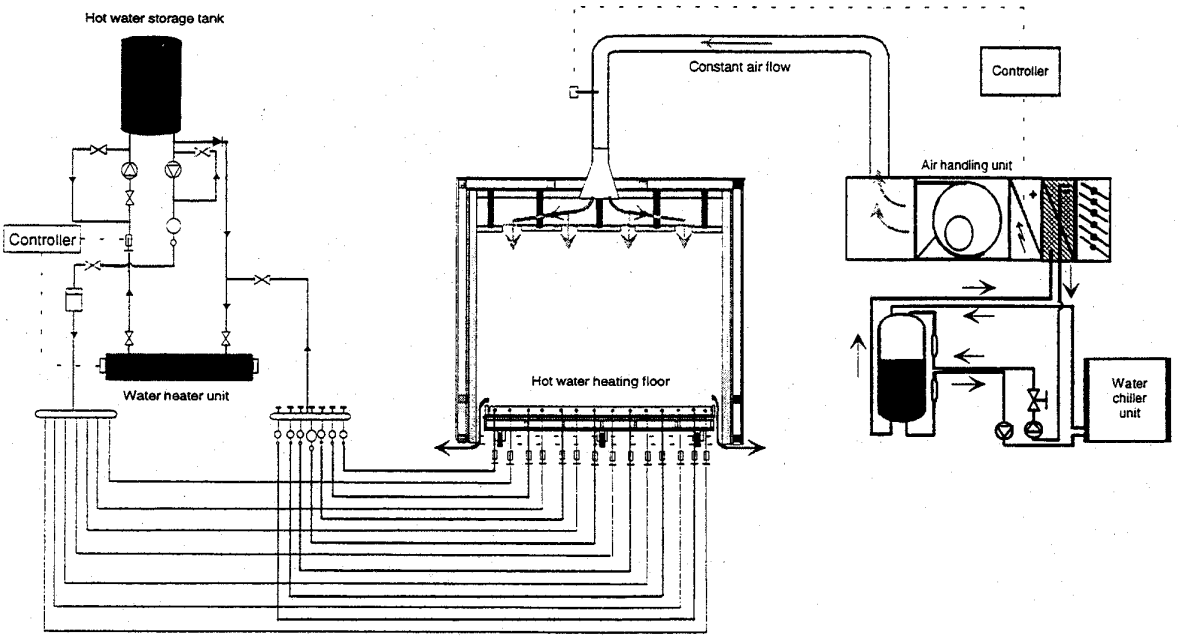

- Figure 1 - Experimental facilities : test-room

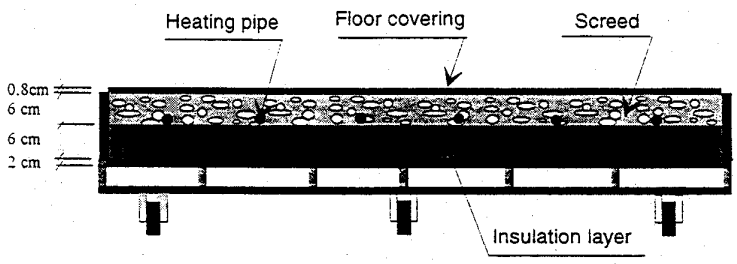

- Figure 2 - Experimental facilities : removable heating floor

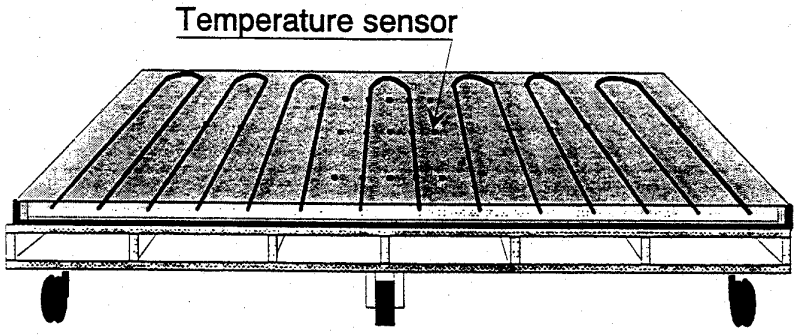

- Figure 3 - General view on the laying of piping

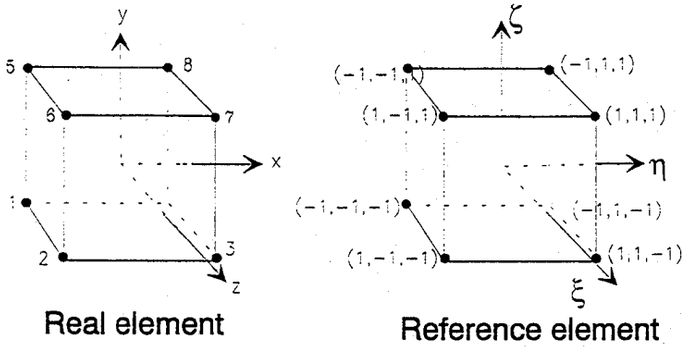

- Figure 4 - Element used for meshing the structure

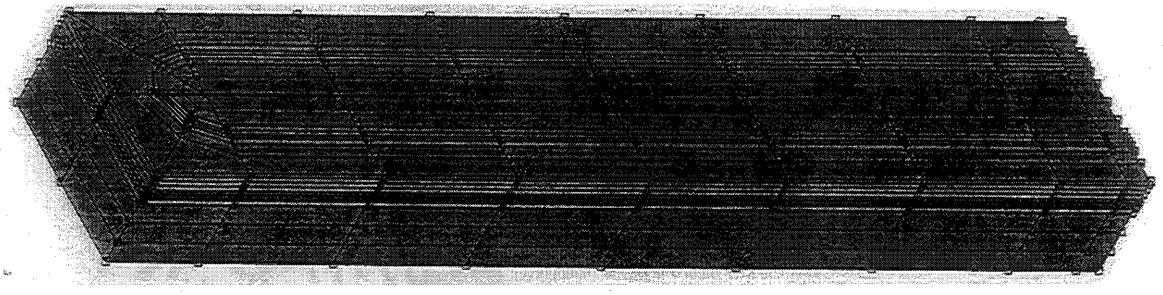

- Figure 5 - Three-dimensional mesh of the structure

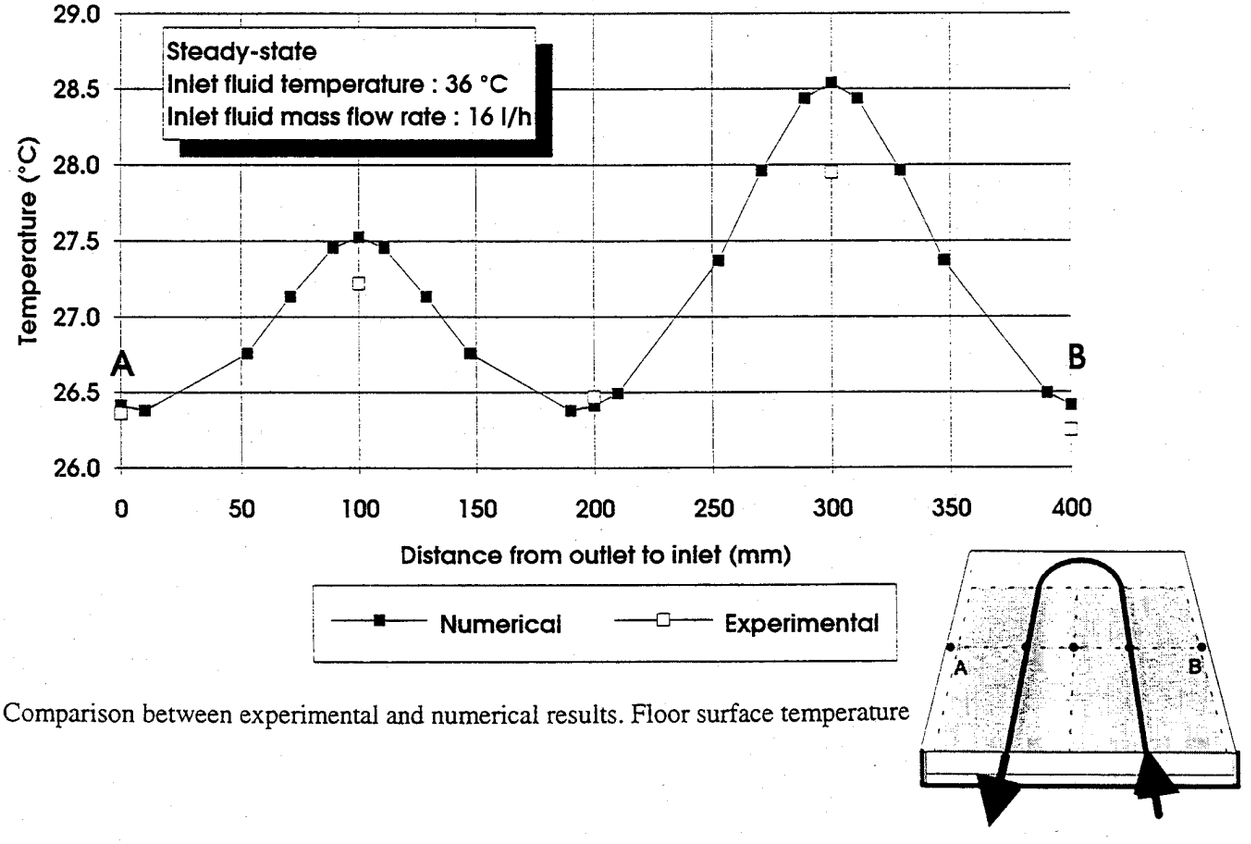

- Figure 6 - Comparison between experimental and numerical results. Floor surface temperature

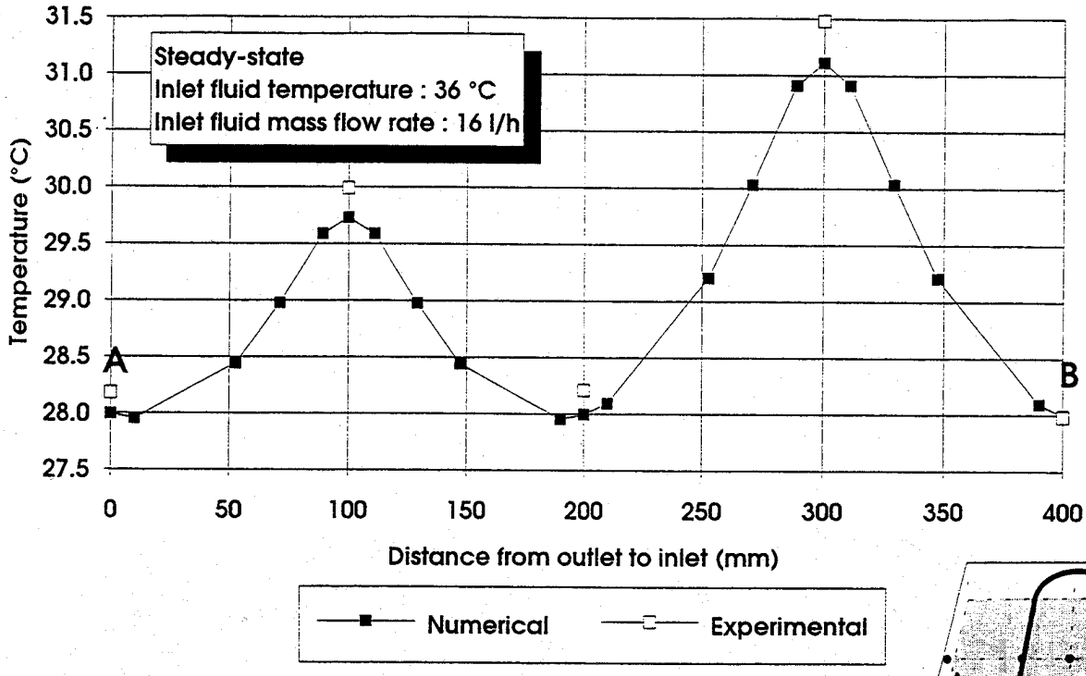

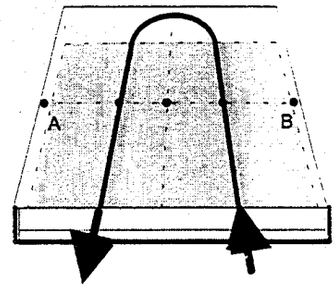

- Figure 7 -

Comparison between experimental and numerical results. Insulation surface temperature

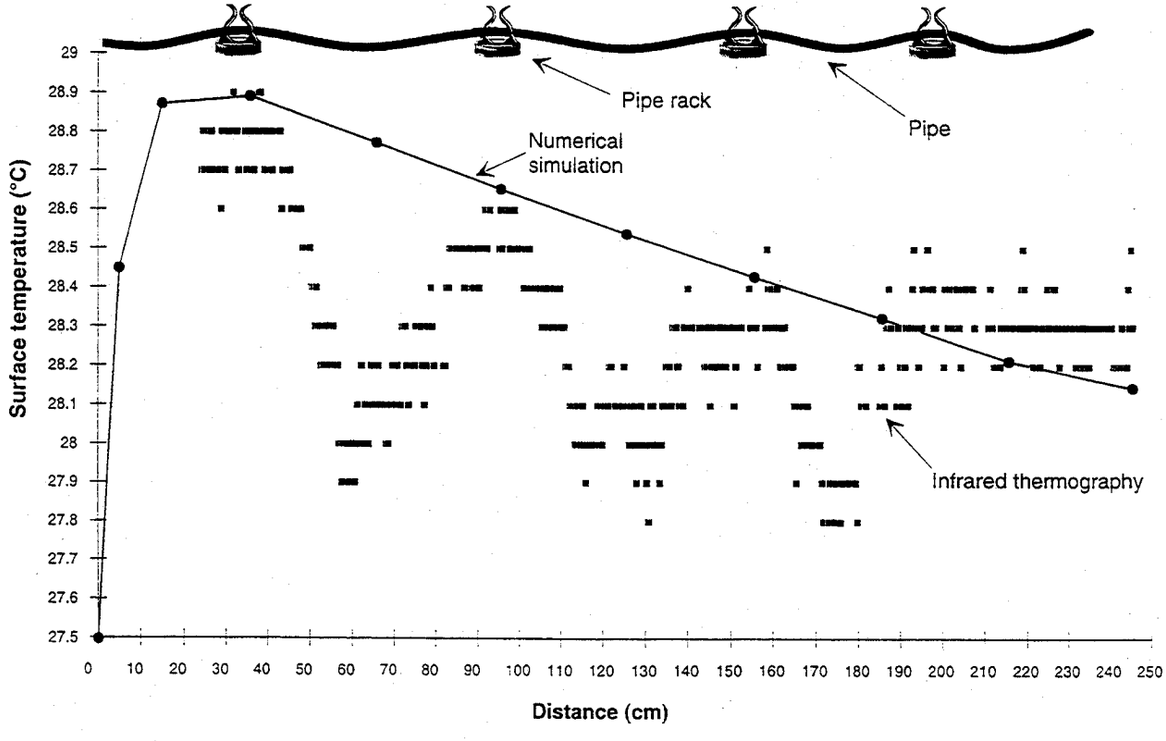

- Figure 8 - Comparison between experimental and numerical results. Influence of the pipe sagging

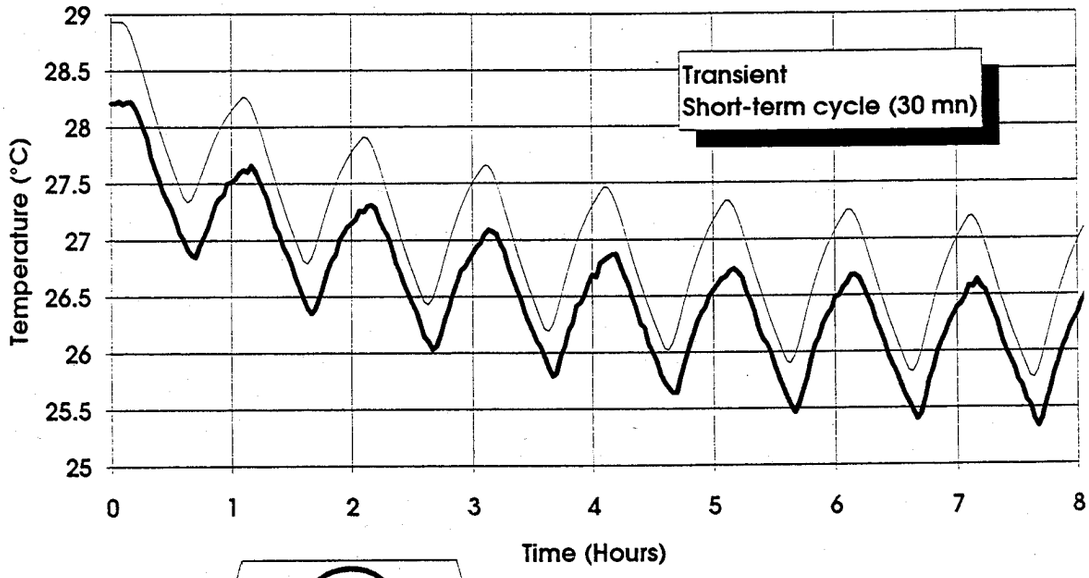

(a)

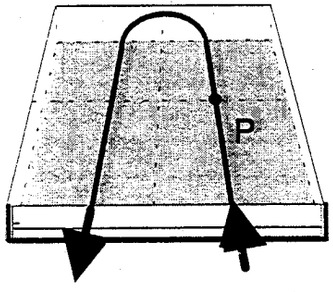

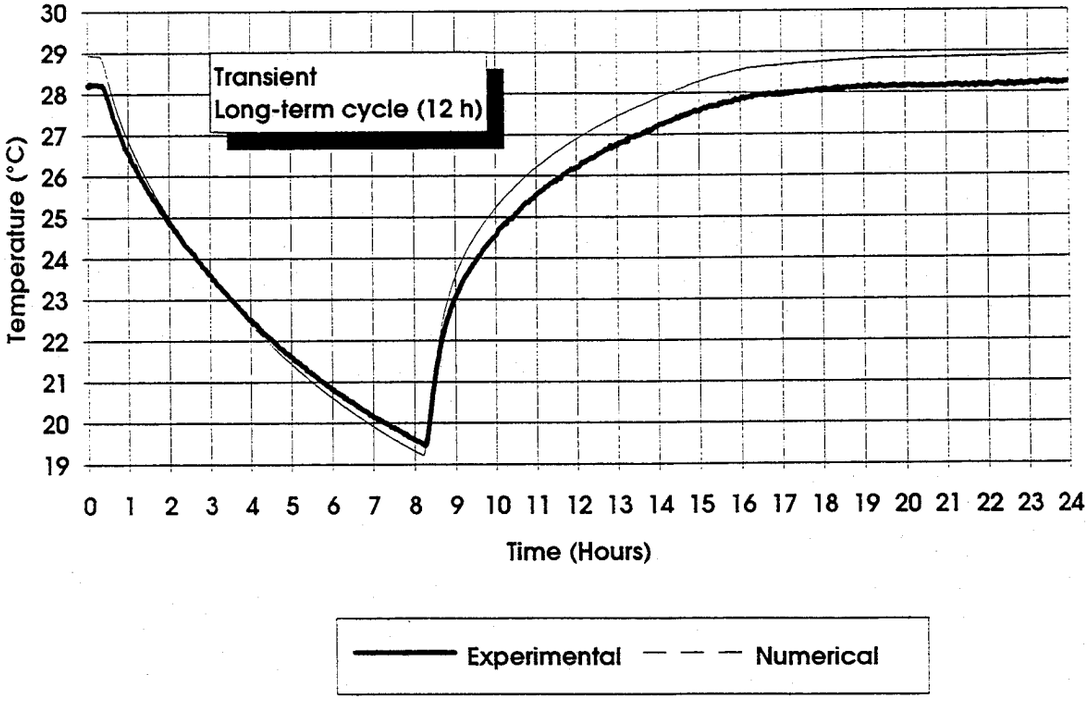

(b)

- Figures 9a et 9b - Comparison between experimental and numerical results. Floor surface temperature at the tracking point P